Laser Science and Technology

Program Update 2002

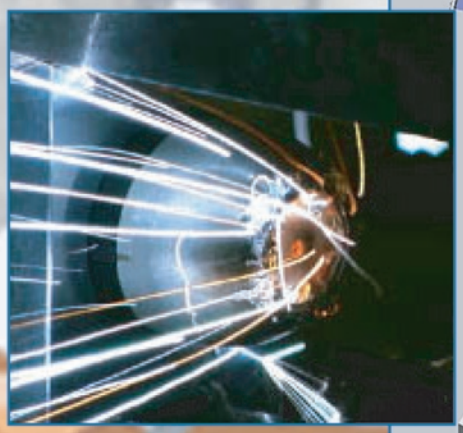

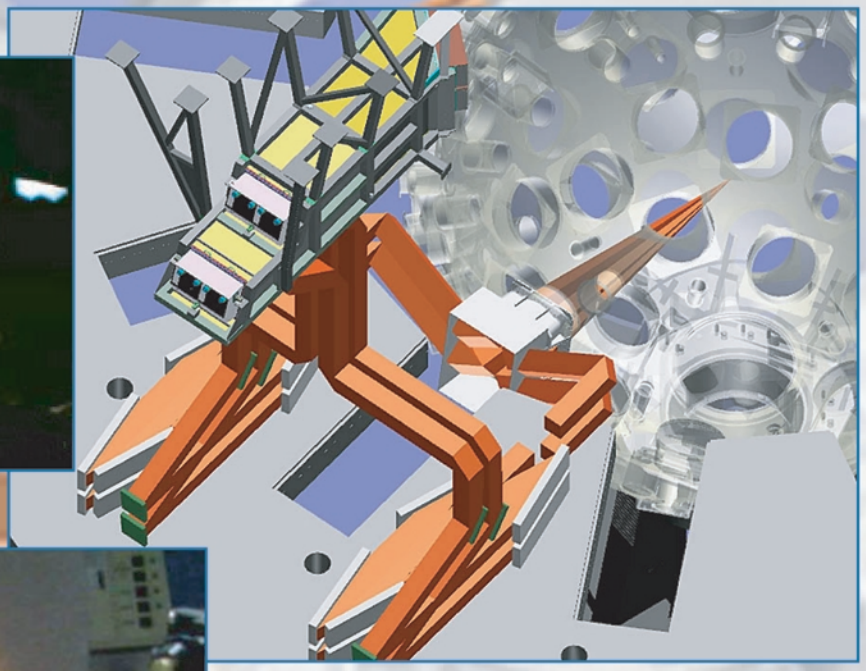

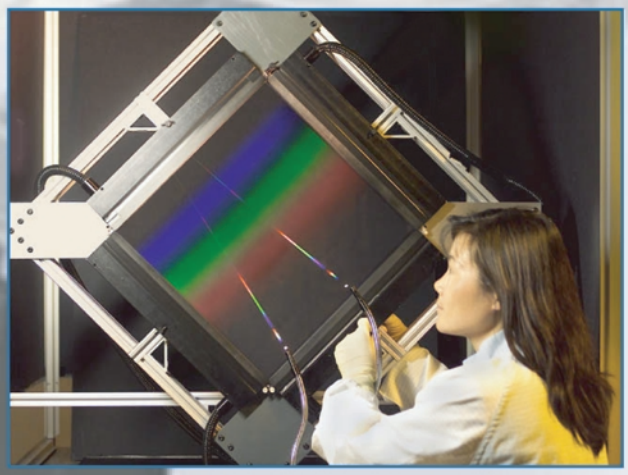

NIF Programs Directorate

LASER SCIENCE AND TECHNOLOGY PROGRAM UPDATE 2002

L. A. HACKEL AND H. L. CHEN

March 2003

LAWRENCE LIVERMORE NATIONAL LABORATORY
University of California • Livermore, California • 94550

TABLE OF CONTENTS

Scientific Editor: Hao-Lin Chen
Publication Editor: Al Miguel
Graphic Designer: Cyndi Brandt

LASER SCIENCE AND TECHNOLOGY PROGRAM

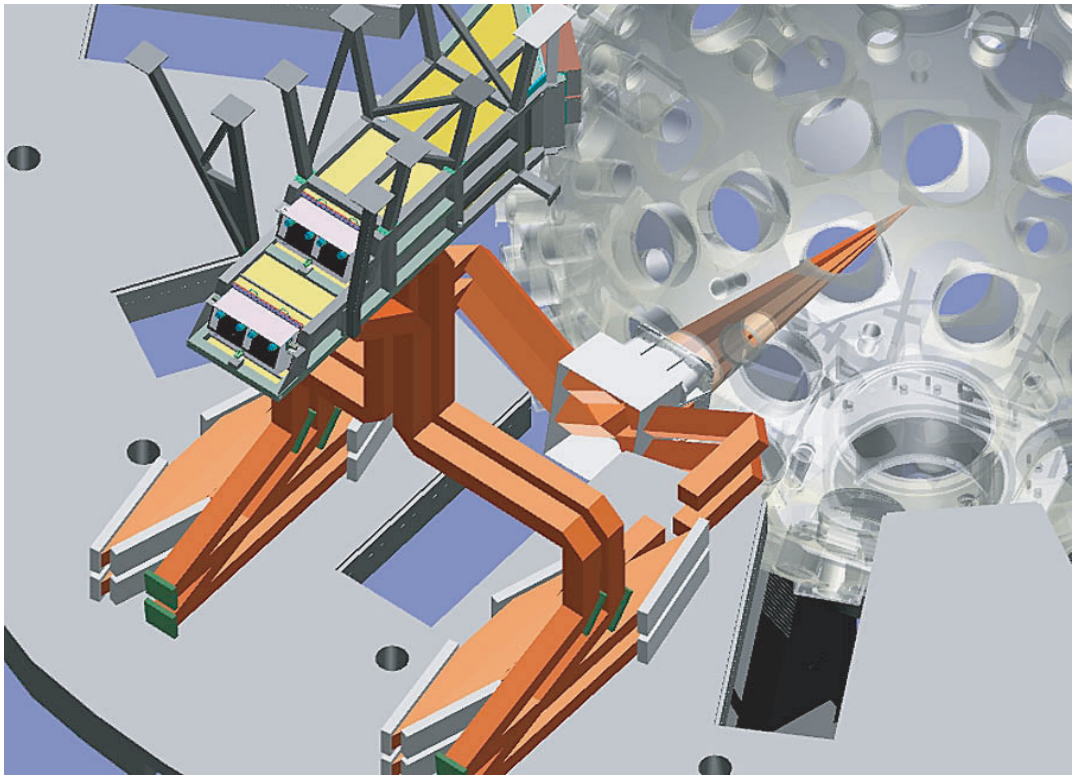

High-energy petawatt laser on NIF simulated in the target bay.

OVERVIEW

The Laser Science and Technology (LS&T) Program's mission is to develop advanced lasers, optics, materials technologies, and applications to solve problems and create new capabilities of importance to the nation and the Laboratory. A top, near-term priority is to provide technical support in the deployment and upgrade of the National Ignition Facility (NIF). Our other program activities synergistically develop technologies that are consistent with the goals of the NIF Directorate and develop state-of-the-art capabilities.

The primary objectives of LS&T activities in 2002 have been fourfold—(a) to support deployment of hardware and to enhance laser and optics performance for NIF, (b) to develop high-energy petawatt laser science and technology for the Department of Energy (DOE), (c) to develop advanced solid-state laser systems and optical components for the Department of Defense (DoD), and (d) to invent, develop, and deliver improved concepts and hardware for other government agencies and industry.

LS&T activities during 2002 focused on seven major areas:

1. NIF Project—LS&T led major advances in the deployment of NIF Final Optics Assembly (FOA) and the development of 3ω optics processing and treatment technologies to enhance NIF's operations and performance capabilities.
2. Stockpile Stewardship Program (SSP)—LS&T personnel continued development of ultrashort-pulse lasers and high-power, large-aperture optics for applications in SSP, extreme-field science and national defense. To enhance the high-energy petawatt

(HEPW) capability in NIF, LS&T continued development of advanced compressor-grating and front-end laser technologies utilizing optical-parametric chirped-pulse amplification (OPCPA).

3. High-energy-density physics and inertial fusion energy—LS&T continued development of kW- to MW-class, diode-pumped, solid-state laser (DPSSL).
4. Department of Defense (DoD)—LS&T continued development of a 100 kW-class solid-state heat-capacity laser (SSHCL) for missile defense.
5. Nuclear energy applications—LS&T continued to develop laser-shock peening technology to improve the service lifetime of metal nuclear waste containment canisters designed for DOE's Yucca Mountain Project.
6. Materials processing—Under cooperative research and development agreements (CRADA) with U.S. industry, LS&T developed and delivered kW-class solid-state lasers for shock peening and hole drilling of metals.
7. Diffractive optics for space telescopes and petawatt lasers—LS&T continued fabrication of large-aperture beam sampling gratings (BSGs) for NIF, and development of large-scale, lightweight diffractive optics for the next generation of space telescope (Eyeglass).

Improving NIF Laser Optics and Material Performance

LS&T work on NIF has achieved major strides leading to the deployment of NIF Final Optics Assembly (FOA) and the development of 3ω optics processing, treatment, and testing technologies to enhance the performance of optics in the FOA. To extend optics lifetimes in the laser chain, we have successfully developed detailed optics processing and treatment procedures. We have completed construction of a preproduction facility (named Phoenix) for conditioning and repairing surface damage on full-scale NIF optics using ultraviolet (UV) and infrared (IR) lasers. We have also upgraded the Optical Sciences Laser (OSL) facility to 1.5 kJ per pulse to perform optical damage tests on 3ω optics for NIF. Ten large-aperture beam-sampling gratings (BSGs) have already been fabricated and four were installed on NIF. We are installing and commissioning a precision diagnostic system (PDS) for the characterization and commissioning of the beamlines during NIF's early light (NEL). We are also improving advanced optical fabrication technologies to fabricate continuous phase plates (CPP) for NIF.

Enhanced Optical Damage Resistance of NIF Optics Using UV and IR Lasers

The output fluences that can be attained on NIF and other megajoule-class solid-state lasers are ultimately limited by laser-induced damage to optical components within the chain. When damage reaches performance-limiting levels, optics must be replaced leading to higher operating expense and longer laser downtime. Because the laser damage threshold of optics decreases with decreasing laser wavelength, the final optics operating at 527 and 351 nm are the most susceptible to damage. The final optics on the NIF consist of frequency-doubling and -tripling crystals fabricated from potassium dihydrogen phosphate (KDP) and deuterated KDP, final focusing lens, BSG, and debris shield fabricated from fused silica. Over the past years, we have developed optic treatment techniques using scanning UV laser beams to condition fused silica optics to increase their damage threshold. We have also demonstrated that CO_2 lasers can be used to stabilize damage sites on optics and control the size of damage sites to less than few tens of microns, thereby greatly increasing the lifetime of an optic through reuse.

With the activation of NIF proceeding, the ability to process full-scale 43-cm × 43-cm optics is timely. We have successfully activated Phoenix to condition and repair surface damage on full-scale NIF optics. This new facility is equipped with two UV conditioning lasers—a 50-Hz Nd:YAG laser operating at 355 nm, with a pulse width of 3.7 ns and a 100-Hz XeF excimer laser operating at 351 nm with 23-ns pulse width. The facility also includes a CO_2 laser for damage mitigation, an optics stage for raster scanning full-scale optics, two microscopes to image damage sites with ≈5-μm resolution, and a damage mapping system (DMS) that can detect damage sites or precursors as small as ≈15 μm to image full-scale optics. The optics are handled in a class 100 clean room

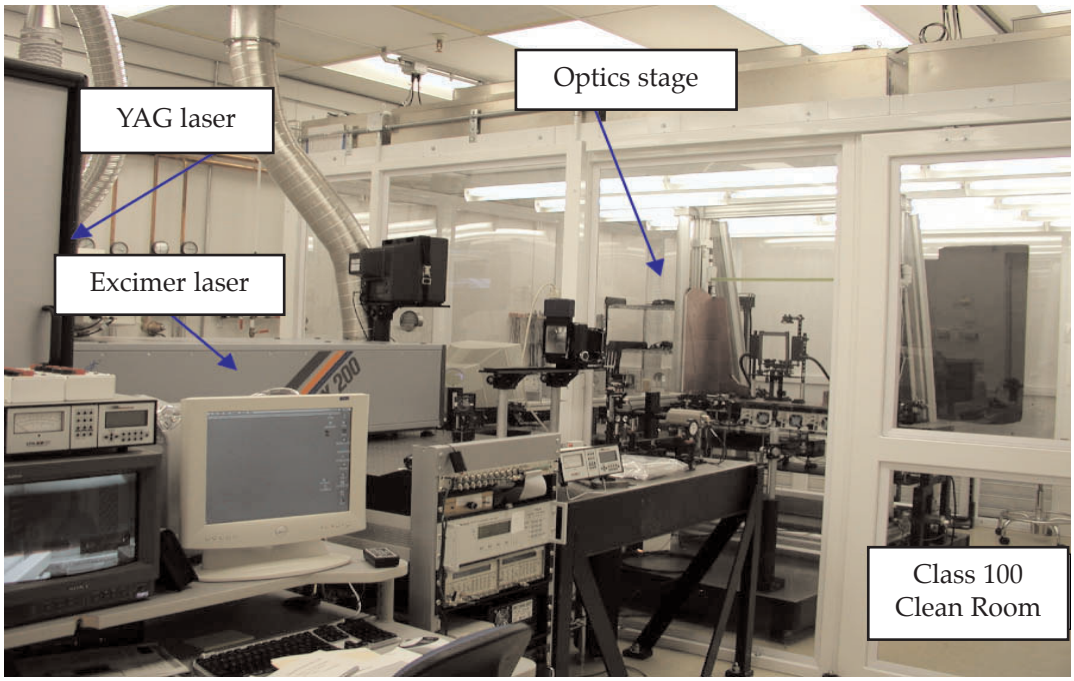

Phoenix, a preproduction facility for conditioning and repairing surface damages on NIF optics.

within the facility that is maintained at better than class 10000.

Three full-scale NIF optics were conditioned in Phoenix, including two wedged final focus lenses fabricated from inclusion-free fused silica. The XeF excimer laser puts out 280 mJ/pulse. It uses a one-dimensional beam homogenizer to tailor the beam profile that converts the 24-mm × 12-mm beam from the laser into a 1.5-mm by 0.3-mm focal spot. Due to the relatively small f-number of the optical system (f/13), the beam cannot be focused at both front and rear surfaces of the optic simultaneously. We thus condition the optic in two steps: output surface first and then the input surface. The first scan is performed at 11 J/cm^2 (which is equivalent to a fluence of 4 J/cm^2 for 3-ns pulses, using $\tau^{0.5}$ scaling). A damage map is acquired to identify new sites or sites that have grown in size. These sites are then spot-treated with the CO_2 laser to eliminate their potential for damage growth. The UV laser treatment process is repeated at 6, 8, and 10 J/cm^2 (all in 3-ns equivalent) for an optic to be used at 6 J/cm^2 and further at 12 and 14 J/cm^2 for an optic destined for 8 J/cm^2 operation. Using UV laser conditioning and IR laser annealing processes, we have been able to maintain <1 defect (or damage site) per fused silica optic at 14 J/cm^2, a 100× improvement compared to last year's result obtained from subscale optics processed in Phoenix. The design goal for 3ω optics is 50 defects per optic. We are designing a production facility to condition and mitigate damage on NIF optics. This facility is planned to be commissioned in 2004.

Qualification of 3ω Optics Using Slab and OSL Lasers

LS&T has established two laser facilities to test FOA optics and certify finishing and post-treatment processes. Optical damage tests on small optics are typically performed using a small laser beam (<1 mm diameter, Gaussian) to raster over the surface of the optics at high repetition rate. To test NIF optics that have relatively large apertures (40 × 40 cm), a large-area, high-energy and high-intensity laser beam that can cover many square millimeters in one shot is required. The OSL and Slab laser facilities were modified to provide such large-area, high-power optical testing capability.

The OSL's 10-cm disk amplifier system delivers up to 12 J/cm^2 of 0.351-μm, 3-ns laser light in a round 3-cm-diameter, flat-top beam at a repetition rate of 2 shots/hour. The flexible pulse shaping and excellent beam quality of this laser make it uniquely suitable for simulating NIF laser conditions on subscale parts of up to 15 cm in size. A main focus during this past year has been the characterization and quantification of surface damage on diamond-turned deuterated potassium dihydrogen

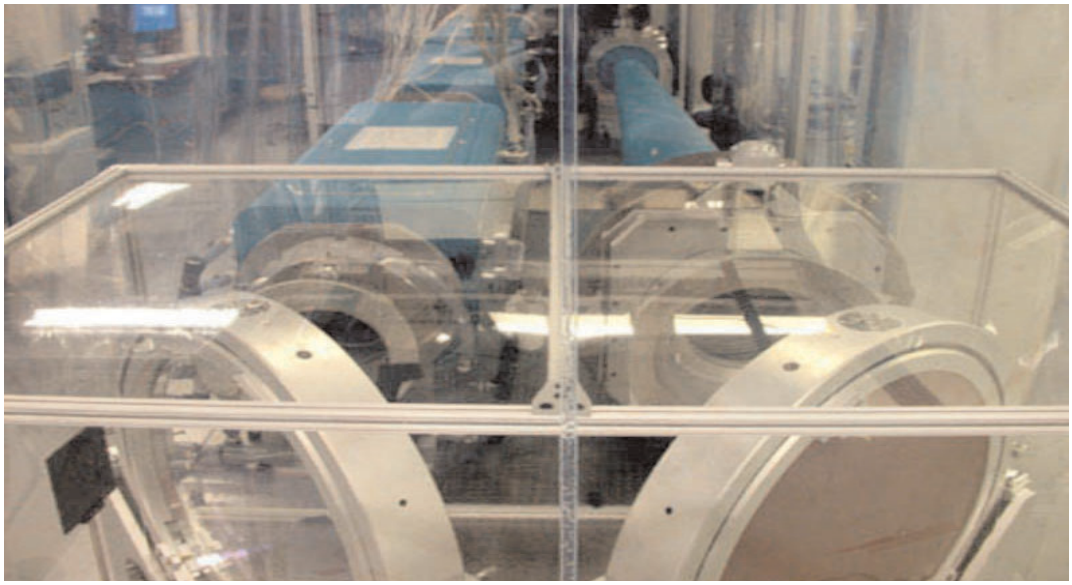

Optical Sciences Laser facility, 20-cm amplifiers on the left and spatial filter telescope on the right.

phosphate (DKDP). Extensive testing of 15-cm material was performed to correlate surface damage to specific defects on the surface of the DKDP (incurred during the diamond finishing process).

The finishing protocol has since been refined to effectively eliminate damage due to these defects. Other work included validation of damage mitigation and stabilization techniques applied to DKDP and fused silica surfaces, validation of small-beam laser conditioning protocols for surface and bulk damage, and the testing of fused silica contaminated with NIF-like shrapnel and target debris for establishing debris shield lifetime.

In 2002, LS&T upgraded the OSL laser to generate 1.5 kJ of 1053-nm light for testing of NIF final optics at full scale. OSL Upgrade uses a double-pass architecture containing four 20-cm aperture disk amplifiers (twelve disks total). The first-article Integrated Optics Module (IOM) has been installed and experiments are under way to verify the frequency converter operation and to test performance at various 3ω fluence levels.

The Slab laser can deliver up to 12 J/cm^2 of 0.351-μm, 11-ns laser light in a square 5-mm flat-top beam at a repetition rate of 30 shots/minute. The repetition rate of this laser enables a NIF lifetime-of-shots to be applied to a test sample in less than a day. Recent work has focused on quantifying the damage growth rate on fused silica surfaces at the individual and combined harmonic wavelengths of Nd:glass, and validating damage mitigation techniques for DKDP surfaces. Current techniques for mitigating damage on the surface of DKDP involve the use of a high-speed diamond-tipped rotary tool to excavate the damage site. The Slab facility has also played an important role in certifying "non-optical" materials for 1ω and 3ω laser exposure. Many engineering applications on the NIF require the use of materials able to withstand diffuse or scattered laser fluences of up to a few joules/cm^2 without generating particles or volatile by-products that can put nearby optical components at risk. Slab experiments were instrumental in providing NIF engineers with a plastic alternative to absorbing glass for protecting the beam transport system from stray 1ω light at fluences up to 1 J/cm^2.

Installation and Activation of the Precision Diagnostic System (PDS) on NIF

LS&T personnel are also commissioning an optical Precision Diagnostic System (PDS) to characterize NIF output beams during the NEL campaign. This system makes use of the 1ω and 3ω diagnostics from Beamlet, where they were used to demonstrate that the NIF laser architecture could produce the 3ω energy and far-field beam quality needed for its missions. The PDS will provide a full complement of 1ω and 3ω diagnostics and make possible the first full-power and full-aperture test of an Individual Optics Module (IOM)—the optical system that mounts directly to the target cham-

ber for each beamline and contains the vacuum window, harmonic conversion crystals, focus lens, diagnostic grating, wave plates, and debris shields. The major components of the PDS consist of turning mirrors that transport the laser beam from the output of the transport spatial filter to the PDS, a roving mirror diagnostic assembly (RMDA) that contains remotely operated robotic handlers and mirrors, a prime focus vessel (PFV), and a target diagnostic chamber (TDC). The TDC is an 8-foot-diameter by 40-foot-long vacuum vessel that contains the beam splitters and down-conversion optics. The entire RMDA enclosure and the beamline to the IOM is sealed and filled with Ar to suppress stimulated rotational Raman scattering during high-power laser shots in PDS. Full activation of the RMDA will allow any one of the 96 beamlines in NIF Switchyard 2 to be transported and analyzed. Commissioning of NIF beamlines using PDS will start in 2003.

HIGH-ENERGY PETAWATT LASER SCIENCES AND TECHNOLOGIES

Development of chirped pulse amplification has made possible production of unprecedented peak power from lasers. With NIF scheduled to produce first light in 2003, there is an increasing interest in the scientific potential of high-energy petawatt (HEPW) pulse production at NIF and other high-energy laser facilities in the U.S. A high-energy petawatt laser initiative has recently been initiated by the DOE to evaluate this frontier technology. LS&T has accomplished a number of major milestones in the development of ultrashort-pulse lasers and high-power, large-aperture optics for applications in SSP, extreme-field science, and national defense.

Petawatt Science and Technology for DOE

With support from the LDRD Program, we are leading an effort to develop a multi-kJ HEPW laser on NIF. The addition of HEPW to NIF will enable the acceleration of data collection for the Stockpile Stewardship Program and new high-energy-density science (HEDS) experiments for advanced inertial confinement fusion (ICF). Several NIF missions benefiting from HEPW capability have been evaluated. These experiments include: fast ignition, high photon energy (10-keV to >10-MeV x-ray) backlighters for large, massive targets, unique Equation of State (EOS) studies, 10- to 50-MeV proton backlighting for electric and magnetic field measurements, ultrahot hohlraums for spectral opacity studies and isochoric heating of inertially confined matter using either the relativistic electrons or ballistically focused protons. Our near-term goal is to develop a 2- to 5-kJ, 5- to 50-ps petawatt laser source for performing HEDS experiments with irradiance in the 10^{19}- to 10^{20}-W/cm^2 range. Our effort in 2002 has focused mainly on designing of advanced laser and optics technologies required to field HEPW beamlines on NIF using existing beamline design for ns-pulse operation. A conceptual design for installing HEPW capability on NIF was completed. To achieve this goal, some modifications to NIF's injection laser system and target areas will be made.

LS&T is developing a stable and correctly phased seed laser as the front end of the HEPW system. We plan to add a short-pulse oscillator and stretcher to the NIF master oscillator room. Output from the oscillator is delivered to a short-pulse preamplifier module to provide a high-contrast chirped pulse for injection to the main NIF amplifier chain. The short-pulse preamplifier module is a line replaceable unit with the capacity to convert from 1 to 4 beams in a NIF quad to short-pulse operation. Dispersion compensation is also added in the preamplifier beam transport system to allow high-order phase adjustment on individual beamlines. To enhance the performance of the Nd-glass laser amplifier, an efficient broadband preamplifier technology utilizing optical parametric chirped-pulse amplification (OPCPA) was developed and evaluated as a possible front end for the HEPW. We are also constructing a compact, ultrahigh-stability, 100-fs mode-locked fiber laser as master oscillator. A large-magnitude, chirped fiber Bragg grating was designed and procured to stretch the seed pulses to multi-nanoseconds. A large-flat-mode (LMF), high-energy (>1-mJ) fiber preamplifier is also being evaluated.

To enable HEPW on NIF, LS&T is also developing high-energy, short-pulse compatible gratings and focusing optics for the back-end system. Four gratings would be used to compensate for both temporal and spatial chirp during pulse compression. Since the laser pulse is shortest and energy is highest on the final

grating and focusing optic, optical damage of these components is a potential problem. Major effort was focused on developing high-damage-resistance, large-aperture multilayer dielectric reflection gratings for compression of the amplified pulses. Initial tests indicate that multilayer dielectric (MLD) coated gratings made with a fused silica (SiO_2) top layer hold promise for high-energy (~5 kJ) operation of a NIF HEPW. The reflection grating developed for HEPW was made with a multilayer stack of dielectric oxides that provide reflectivity at wavelength and angle of use and a SiO_2 grating layer with width and height of grooves designed for maximum efficiency and lowest electric field structure at a specific incidence angle. Using photoresist and holographic exposure tools and a large-area ion beam etcher, we were able to generate the grating grooves with high precision. The key to high-damage-fluence MLD gratings is to minimize the E-field enhancement at the groove surface. We are currently fabricating and damage testing sample gratings compatible with kJ-level short pulse production. Our goal is to build 2-meter aperture grating structure with 75% compressor efficiency and individual grating efficiency >94%. A schematic of the pulse compressors and parabolic focusing optics is shown in the figure (orange color) on page 1.

Generation of X-Rays by Thomson Scattering between an Ultrashort Laser Pulse and a Picosecond Electron Bunch

With funding from the LDRD Program and in partnership with the Physics and Advanced Technologies (PAT) and the Engineering Directorates, LS&T continues to develop an ultrafast x-ray source based on Thomson scattering of fs laser pulses from relativistic-electron bunches from a linear accelerator (linac). After years of intensive R&D, the experimental setup for Thomson scattering is returning results. In recent experiments, we successfully generated 70-keV x-rays with extremely high brightness. The immediate application of this intense x-ray source (20–100 keV) will be in pump-probe experiments for the Stockpile Stewardship Program to temporally resolve structural dynamics and atomic motion in high-Z materials with ps-resolution.

The PLEIADES facility (Picosecond Laser Electron InterAction for Dynamic Evaluation of Structures) is located in Bldg.194 where PAT's high current, rf, electron linac and LS&T's fs-laser facility (FALCON, femtosecond accelerator laser concept) are installed. We have recently completed construction and synchronization of a dual-beam Ti-sapphire laser

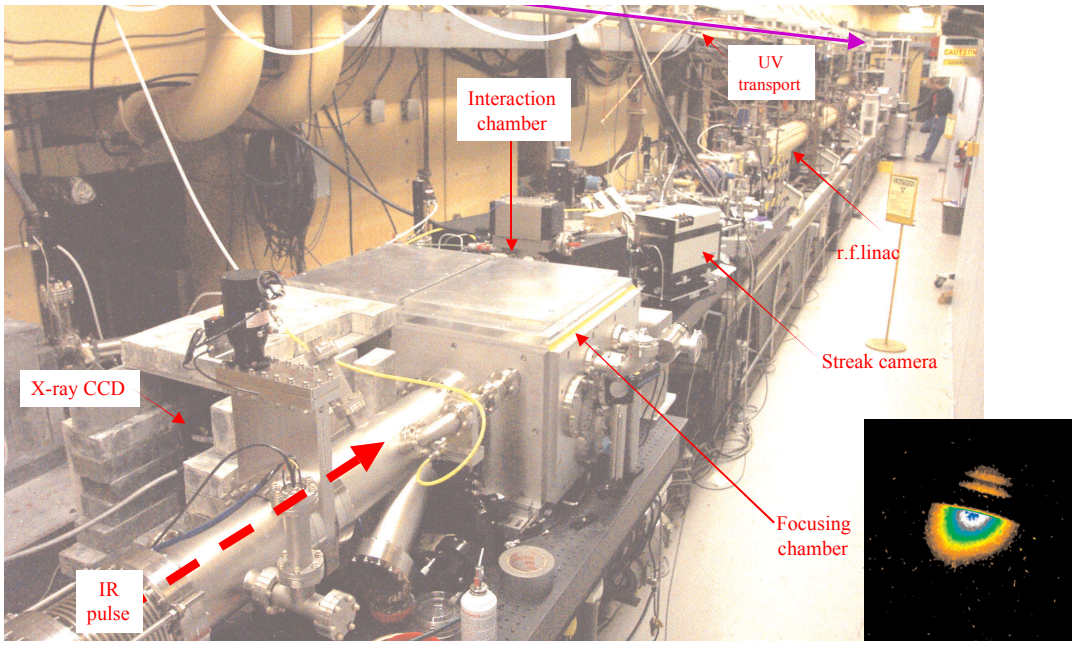

Short-pulse Thomson x-ray source. IR laser photons scatter off electron bunch in the interaction chamber located in Bldg. 194 where LS&T's fs-TW laser facility and PAT's electron linac are located. An x-ray image from a Thomson CCD camera is also shown. Top of beam is occluded by x-ray photodiode.

system for photon-electron counterpropagation experiments. A single, mode-locked oscillator is used to seed both the main IR laser system (the source of fs photons) and the photoinjector laser system (PLS, which seeds the linac). The laser master oscillator is phase-locked to an rf crystal oscillator to drive the klystrons that power the linac. The PLS consists of a regenerative amplifier (regen) and single 4-pass amplifier that yields an IR output of ~100 mJ. The amplifier output pulse is compressed using a small, dual grating compressor. The compressor output pulse is frequency-tripled to 266 nm and transported to the photogun to produce photoelectrons from a polished copper cathode. The photoelectrons are accelerated to 5 MeV and injected into the linac and accelerated between 50 to 80 MeV.

In the main IR laser, after the grating stretcher, the 600-ps pulse is amplified to 1 J by three stages: a regen, a 4-pass-preamplifier and a second 4-pass power amplifier, and then transported to a vacuum grating compressor. The 600-ps, 1-J pulse is compressed to ~50 fs and propagated (in vacuum) to the interaction region. Inside the interaction chamber, the electron pulse is focused by a magnetic lens to a 50-μm spot. The laser pulse is delivered and focused to the same interaction point from the opposite direction to collide with the electron bunch at an ~180° angle.

In the scattering chamber, the laser photon energy, E_L, is upshifted by an amount proportional to the square of the relativistic energy of the electrons. In our current experimental arrangement, the electron energy is 54 MeV, the energy of 800-nm photons (E_L) is 1.55 eV, and so the energy of x-ray photons (E_x) is calculated to be 70 keV. Initial experiments were performed with the laser pulse and electrons interacting head-on. We are also designing experiments for 90° scattering between the electrons and photons, which will produce subpicosecond x-ray pulses.

Several diagnostic tools were developed to monitor the Thomson x-rays. The image of the Thomson x-ray beam monitored by an x-ray charge-coupled device (ccd) camera was also recorded. The top portion of the beam was occluded by one of the x-ray photodiode packages. The estimated x-ray flux for this shot was 10^5 photons at an average energy of 70 keV. This is the highest single-pulse ps x-ray flux ever produced at this energy. Two other groups, one at LBL and the other in Japan, have produced comparable x-ray fluxes at lower energy, 30 keV and 14 keV respectively. With straightforward improvements to the laser focal fluence and focused electron spot, we expect an ~1000-fold improvement in the x-ray flux in future experiments.

Short-Pulse, High-Average-Power Laser System for Micromachining

Under a work-for-others contract, LS&T is developing a 100-W class picosecond, kHz, solid-state laser system for rapid, precision drilling of small (μm-scale) holes in metal and alloys. We have recently completed the assembly and initial testing of this advanced laser drilling system and were able to deliver over 35 W in a 2-ps, 4-kHz pulse train to the workpiece for material processing application.

Below: Large dielectric diffraction grating used in the 50-W-psec-pulse machining laser has a diffraction efficiency of 97% and rms wavefront of 1/40th of a wave.

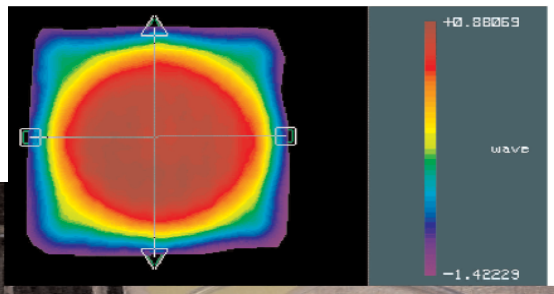

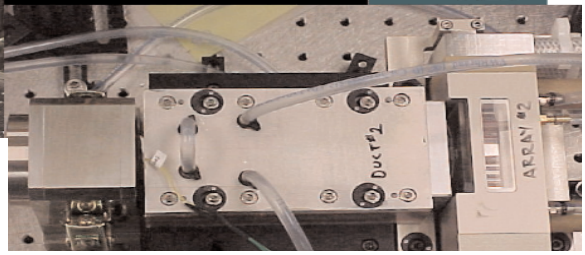

Lower right: Diode-pumped CPA uses hollow lens duct and end-pumped power amplifier and a wet-etched ultrathin phase plate to format beam (upper right).

This short-pulse, high-average-power laser employs numerous advanced technologies of the LS&T program. These technologies include fiber mode-locked oscillators, solid-state regenerative and power chirped-pulse amplifiers using diode-pumped Yb:YAG as the gain medium, and a high-power multilayer dielectric grating. The laser system architecture is based on chirped-pulse amplification (CPA). It starts with a mode-locked Yb-doped fiber laser, which was developed by Imra Corporation specifically for this application. This mode-locked oscillator produces 8-psec pulse trains and has an average power of 120 mW (2.4 nJ/pulse at 50 MHz). The spectral bandwidth of the oscillator pulses is 2 nm. The psec pulses from the fiber oscillator are stretched in time to 2 nsec using a diffraction grating pulse stretcher, amplified by 90 dB, then recompressed to 2-psec duration before being sent to the target chamber. Between each of these laser subsystems, we use computer-based pointing and centering loops to precisely control laser beam alignment.

The stretching-and-compressing process that is the crux of the CPA architecture is accomplished using a high-efficiency dielectric diffraction grating manufactured by LS&T's Diffractive Optics Group. This large (150 × 335 mm^2) multilayer dielectric grating has a diffraction efficiency of >97% at 1030 nm. Whereas a typical CPA-based laser system architecture may use 4 diffraction gratings (2 for the stretcher and 2 for the compressor), the current design employs a single grating that is shared by both the stretcher and compressor.

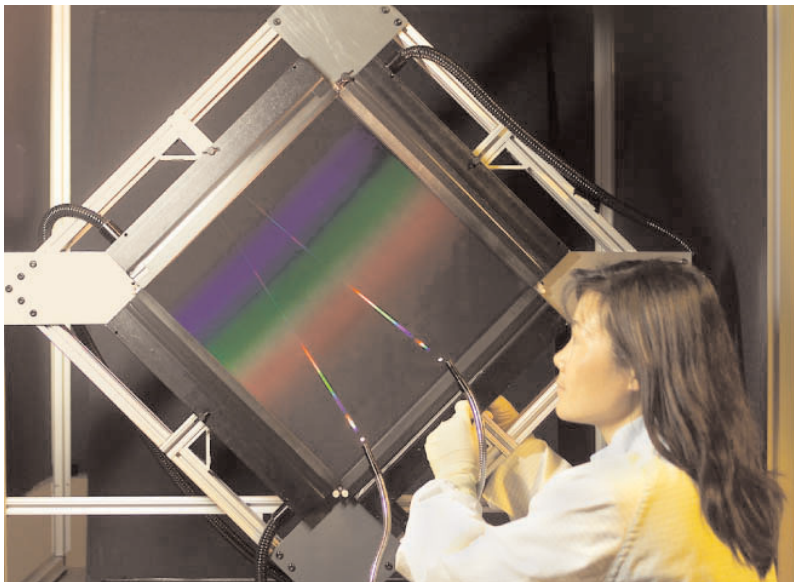

Large fused silica Beam Sampling Grating fabricated for NIF.

This single-grating stretcher/compressor design enabled us to combine two of the laser subsystems in a compact unit that can readily be incorporated into a hardened system that can withstand the harsh conditions typically encountered on the factory floor. The 90 dB of amplification between the pulse stretcher and compressor is accomplished by two subsystems: a linear-cavity regenerative amplifier and a power amplifier. Both amplifiers use Yb-YAG as the gain medium, and the power amplifier is pumped with microchannel-cooled diode laser arrays (operated at 940 nm). The regen amplifies the 1-nJ stretched pulses up to 750 μJ and converts the pulsing frequency from 50 MHz to 4 kHz (using a Pockels cell). The power amplifier has two heads. It boosts the regen output from 3 W to 50 W in two passes. With the use of a grating compressor, the pulse width of the amplified beam from the power amplifier is compressed from 2 ns back to 2 psec, multiplying the laser peak power by a factor of a thousand.

For drilling or material processing, the output from the compressor is delivered directly to the workpiece in the target chamber. Online beam diagnostics are developed to record and control the output power, beam quality, and wavefront of the laser. We have made good progress in the drilling of sub-μm holes in metals and alloys as required by our industrial partner. Under the support of ICF's Target Science and Technologies group, we have also built a new cutting station and coupled to an existing short-pulse machining laser to drill high-aspect-ratio, micron-scale holes for fusion target fabrication. Early trials of the system have demonstrated the feasibility of drilling holes that extend more than 100 times beyond the system's Rayleigh range. Holes with 3-μm diameter have been drilled in 125-μm-thick Be and Al foils as well as thin-walled Be capsules.

Fabrication of Beam Sampling Gratings (BSGs) for Power Balancing of NIF Laser Beams

Balancing the power on all the NIF beams requires a precise power measurement on each individual beam. This measurement has to be stable to ±1% over a period of time and should

be directly relatable to the energy on target without additional ambiguities or uncertainties. This requires that the measurement be done as close to the end of the laser chain as possible. Using a Fresnel reflection off an optical surface does not provide the required stability because the antireflection coatings degrade over a period of time, and because a reflected sample beam does not travel through all of the optical surfaces. A transmissive diffraction grating inserted in the beam path provides a stable sample of the beam for the power measurements. The requirements on this beam sampling grating for NIF are that the grating diffract in transmission a small fraction (~0.3%) of the incident high-power laser beam and bring it to focus at a distance of approximately 1.2 m from the optic. This requires a shallow grating structure (~15 to 20 nm deep) with concentric grooves. The grating period ranges from 1 to 3 μm. LS&T personnel assembled a wet-chemical processing machine and a patterning-and-illumination station to fabricate full-size BSGs with 5- to 30-nm groove depth for power balance diagnostics on NIF. We have completed building and testing of production hardware for fabricating BSGs. Ten full-aperture fused silica BSGs have been fabricated for use on the NIF to be used on NIF early light campaign.

Development of Continuous Phase Plates for NIF with Wet-Etch Figuring

With support from the Laboratory Directed Research and Development (LDRD) Program, we continued to develop a low-cost wet-etching tool for precision optical figuring and finishing of full-aperture optics for NIF. Wet-etch figuring (WEF), is a method for generating arbitrarily shaped optical surfaces using wet chemical etching. During the fabrication process, the etching region on the optic is confined to a stable droplet size through the use of surface tension gradients (called Marangoni confinement), and is moved in a controlled fashion over the optic surface to precisely generate the desired optical figure on very thin glass substrates. Real-time measurement of the surface wavefront during the etching process and feedback allows for a close-loop figuring operation. Over the course of this year, we further refined the process and applied it to fabricate subscale continuous phase plates (CPPs) for testing. A small-aperture (30- × 30-mm) CPP was fabricated on 1-mm-thick borosilicate substrates. This optic is designed as a beam homogenizer to generate a smooth, super-Gaussian focal spot at target. The surface height gradients for this optic are 0.5 μm/mm. Our ultimate goal is to produce full-aperture (40-cm × 40-cm) CPPs for NIF in the future. For precision material processing using short-pulse lasers, we have also fabricated ultrathin (1-mm) phase plates for modifying the focal spot on the workpiece.

FABRICATION OF A 5-m-DIAMETER DIFFRACTIVE FRESNEL LENS FOR SPACE-BASED APPLICATIONS

Detection and imaging of distant objects, such as the exosolar (outside our solar system) planets, require optical telescopes with large-aperture primary optics. Large apertures gather

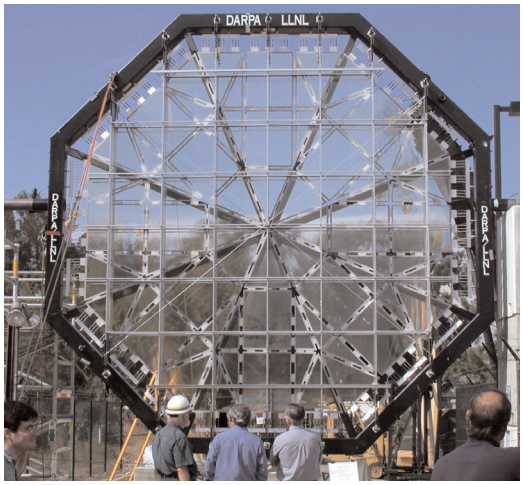

Five-meter foldable, ultrathin, lightweight Fresnel lens for space-based applications.

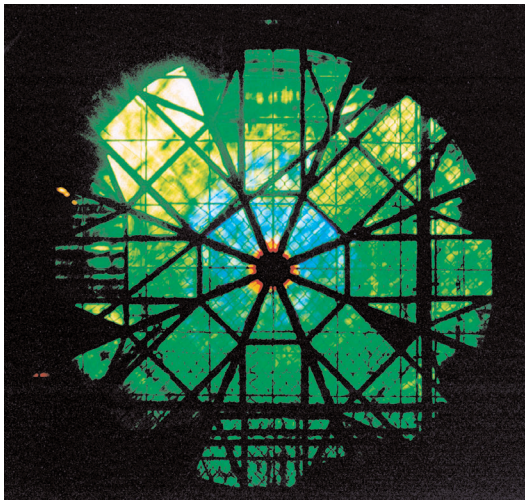

Focal spot produced by the 5-m Fresnel lens when illuminated with 532-nm light. Inscribed is a 2.5-cm-diameter circle. The central portion of the image is saturated.

more light from these objects, thereby increasing the signal-to-noise ratio. Space deployment of such telescopes severely limits the weight of the optical components and requires that the primary optic be thin, lightweight, and compact for deployment. Transmissive optics (lenses) are less sensitive to surface ripples and pointing errors than reflective optics (mirrors). Lenses can be made lightweight by replacing conventional lenses with diffractive Fresnel lenses.

Funded by LDRD, LS&T continues to develop large-aperture Fresnel lenses for space telescopes (Eyeglass project). In an early effort, we built diffractive telescopes at apertures up to 20 cm diameter and demonstrated their color-corrected operation over a 470- to 700-nm-wide bandwidth. We also successfully built large-aperture, space-deployable optics that can be packaged into a small volume for launch. For our first assembly, we built a 75-cm-diameter Fresnel lens made up of six segments and assembled it using 2.5-cm-wide metal hinges. After fabrication, this lens was shown to produce a diffraction-limited focal spot unaffected by folding and unfolding operations.

To further demonstrate the feasibility of scaling this concept to larger sizes, we have recently built and operated a 5-m-diameter Fresnel lens. This lens consists of 72 segments of 0.7-mm-thick glass panels that are glued together using 5-cm-wide metal hinges. The particular layout of the pattern was chosen to allow the lens to be folded into a cylinder of ~1/3 its diameter. The glass panels used for this lens are mass produced for flat-panel displays, making them very inexpensive. Optical testing consisted of hoisting the lens in a vertical position (see top photo on page 1-9), illuminating it with monochromatic light from a laser and observing the focal spot produced by the lens. We successfully tested the lens at 405-, 532-, and 670-nm wavelengths. The focal spot size and shape are dominated by the aberrations inherent in the glass panels and the reduced precision in the alignment of the panels. Both these limitations will be overcome in the future.

Advanced Solid-State Lasers and Components

LS&T provided development and expertise for a number of DOE and DoD projects. These include developing advanced 100-kW-class high-power diode-laser arrays for the Mercury laser and Solid-State Heat-Capacity Laser (SSHCL) projects, developing advanced fiber lasers for petawatt and laser guide star applications, building high-energy lasers in collaboration with PAT and the University of Nevada, Reno, activating x-ray ablation experiments to evaluate IFE optics, and beginning activation of the Mercury laser. Mercury is a kW-class, diode-pumped, solid-state laser (DPSSL), intended to serve as driver for high-energy-density physics and inertial fusion energy.

Mercury Laser: a Diode-Pumped, Gas-Cooled, Solid-State Slab Laser for Inertial Fusion Energy (IFE)

Diode-pumped solid-state lasers are one of four driver technologies being considered for inertial fusion energy power plants. Each driver development project, including solid-state laser, heavy ions, Z-pinch and gas laser (KrF), is currently focused on demonstrating several proof-of-principle design concepts. The Mercury laser is being activated and will test key technologies including high-power laser diodes, crystals, and gas cooling within an architecture that is modular and scalable to multi-kilojoule apertures with minimal beamline reengineering.

The design requirements of the laser are to operate at 10 Hz and 100 J/shot within a 10% efficiency envelope. To meet this goal, we explored numerous gain materials and architectural options to best fit the design space of a fusion energy class laser. $Yb^{3+}:Sr_5(PO_4)_3F$ or Yb:S-FAP was chosen as the gain medium based on its long energy storage lifetime, moderately high cross section, and good thermal conductivity. The primary challenge has been in growing large aperture slabs of 4×6 cm^2 in area. However, the growth techniques employed to eliminate or reduce the crystalline defects produced boules that were difficult to cut due to the high thermal gradients required during the growth process. Using stress models developed in conjunction with a research group at the University of California, Davis, we chose an off-center cut geometry with a high-pressure water jet to overcome the high probability of boule-fracture during fabrication. This method has proven successful and five S-FAP slabs have been mounted onto the first amplifier. Four additional slabs are in fabrication and seven crystalline boules are waiting to be cut. The slabs are mounted onto aerodynamic aluminum structures called “vanes” that are separated by

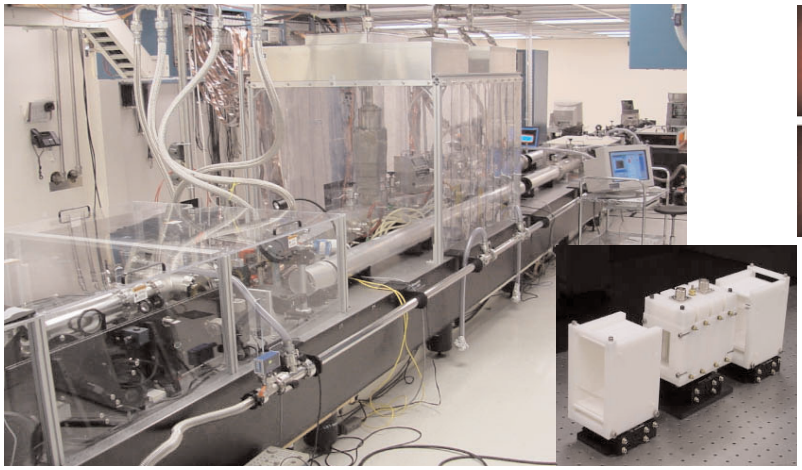

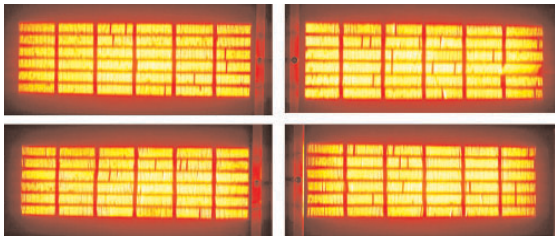

Left: Mercury laser—gas-cooled amplifier head, pump delivery, and diode array. Upper right: Four 80-kW diode backplanes have been built and tested in the Mercury laboratory. Center inset: 100-W Pockels cells have been fabricated and installed in the laser.

1-mm helium gas cooling channels. Recent measurements of Yb:S-FAP indicate damage thresholds of greater than 30 J/cm^2.

The laser diodes at 900 nm are precision mounted onto etched silicon heatsinks with microlenses to help reduce the light divergence, and then secured onto large copper blocks or arrays that provide the cooling and electrical power to the diodes. Each amplifier assembly is pumped by four 80-kW diode arrays. Four arrays have already been built and are currently being exercised in the system. Together they have accumulated over 10^5 shots. Several sets of diode array backplanes have been qualified and will be used for the second amplifier assembly. The diode array light is guided to the amplifier through multiple reflections within a hollow lens duct and homogenizer.

The amplifier was assembled with five Yb:S-FAP slabs and two undoped glass slabs. The undoped slabs serve as placeholders in the amplifier until the remaining S-FAP slabs can be fabricated. With 200 mJ of injected energy, we were able to extract up to 31.6 J of energy at 1.047 μm in single-shot mode. At 10 Hz, we measured an average energy of 20.6 J. Wavefront data was taken for static (no diode pumping) and full pumping conditions. The static wavefront data show 2.7 waves of peak distortion due to bonding phase discontinuities incurred during the fabrication process. New fabrication techniques are being tested to eliminate these distortions. In the interim, a static conjugate phase plate, using the wet-etch technology developed by LS&T, was used to correct for the distortion when placed directly adjacent to the amplifier assembly. We measured a factor of three improvement in the energy within a diffraction-limited spot for unpumped conditions. The conjugate phase plate will be used in the system until the slabs can be replaced with ones with higher optical quality.

The overall architecture employs an angularly multiplexed, four-pass beam layout. Relay imaging of the laser beam with telescopes between the amplifiers helps to greatly reduce the intensity modulation at the crystalline amplifiers. A100-W, large-aperture birefringence-compensated Pockels cell is used after two passes at low fluence (<1 J/cm^2) to help suppress parasitic beams. The laser system, diode laser power conditioning, and utilities are computer controlled. A full suite of sensor packages is used to diagnose the beam after

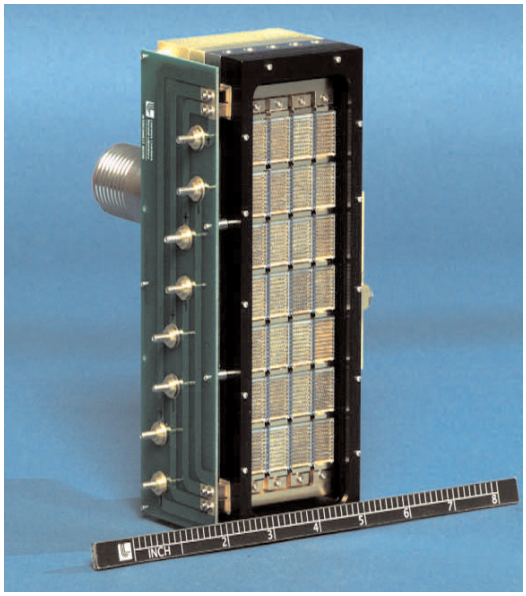

Pump module constructed from 28 closely packed SiMMs tiles arrayed in 4 rows of 7 tiles. This pump module is designed to deliver 42 kW of pump radiation.

each pass. A dark field diagnostic allows detection of damage on every shot such that when a damage site >100-μm is detected in the dark field image, the laser is shut down immediately. Future plans include installation of the remaining two S-FAP slabs in the first amplifier head, followed by single-amplifier experiments and then activation of the second amplifier. When complete, Mercury laser will yield up to 100 J /pulse at 10 Hz.

Fabrication of 100-kW-Class Laser Diode Arrays for Optical Pumping of Lasers

LS&T continues to develop diode laser arrays packaging technologies for optical pumping of kW-class and heat-capacity lasers. In 2002, we fabricated two 42-kW peak-power packaged arrays for the solid-state heat-capacity laser (SSHCL) and eight 80-kW packaged arrays (backplanes) for Mercury laser projects.

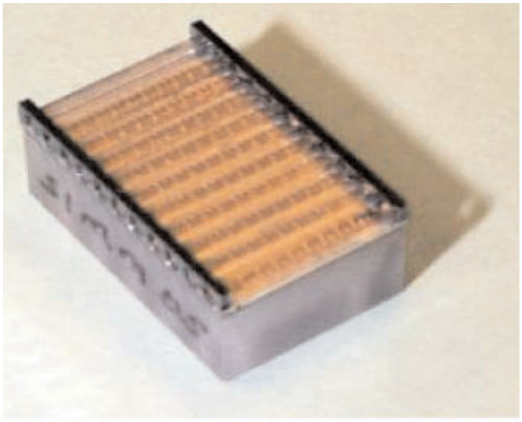

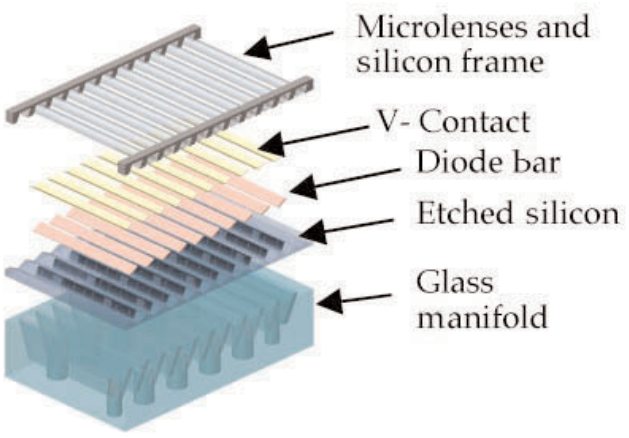

The SiMMs package holds 10 individual laser diode bars in a single monolithically cooled silicon tile. Top: Photograph of an individual SiMMs package. Bottom: Assembly drawing showing the various SiMMs package components in an exploded view.

To imagine 100-kW diode arrays becoming a common reality, two key elements of the technology need to fall into place: (1) high-performance, reliable diode bars and (2) heatsinks that offer excellent thermal management and precision diode bar mounting. Rapid cooling of diode laser arrays is achieved using silicon microchannels. Photolithography and etching techniques are applied to produce tens of thousands of 30-micron-wide channels in silicon substrates. Water flowing through these microchannels aggressively cools the laser diode bars, which are mounted on the silicon at location less than 200 microns from the channels. By combining 10 diode bars onto a single heatsink, a 10-bar package, referenced as a tile, serves as the unit cell from which large two-dimensional diode arrays can be built up through tiling. We have recently completed packaging of several diode arrays. Each package is capable of generating in excess of 40 kW of optical power. Noteworthy is that the brightness (i.e., W/cm^2-str) of the array is extremely high, by virtue of the compact tiling of the heatsinks and the precision placement of 10-element microlens arrays on each tile.

The individual tiles that are used to make up these large arrays are called SiMMs for Silicon Monolithic Microchannels. The considerations that drove the SiMMs package design were ease of fabrication and the ability to construct large laser diode arrays with output power capabilities of 10 to 100 kW. Of paramount importance in the design of the SiMMs package was the requirement that the same aggressive heat removal capability that characterized our original rack-and-stack silicon microchannel-cooled package be preserved in the SiMMs. This requirement was met by incorporating microchannels into the silicon directly below the location of the attached laser diode bars. The SiMMs design has a very tight thermal circuit with only 177 microns of silicon separating the heat-generating laser diode bars and the microchannel fins that define the cooling channels.

Since almost all applications at LLNL now require microlensed arrays, the development of an easy and efficient microlensing attachment technology was an important consideration during the design phase of the SiMMs package. Easy and efficient microlens attachment translated into a requirement that an entire SiMMs

package be microlensed in a single step. Single-step microlensing of an entire tile eliminates the production steps necessary to individually attach a microlens to each diode bar as we do in our rack-and-stack package. From our previous experience with the rack-and-stack package, we know that microlenses must be placed with a positional tolerance of a few microns relative to the diode bar emitter facets to achieve good optical performance. This implies that the single-step microlensing of an entire SiMMs tile will require the individual diode bars within a tile be positioned relative to one another with at least the same few-micron accuracy.

The precision placement of the laser diode bars on the SiMMs package is accomplished by using a V-groove technology on the front surface of the package. These V-grooves are generated using the same etching technology that is used to fabricate the microchannels into the backside of the silicon. The emission direction of the diodes at 55° to the normal of the SiMMs front face is due to the orientation of the V-grooves that serve as pads for the laser diode bars. With the diode bars precision located, the microlenses can be held in precision frames fabricated in the form of silicon runners using the same anisotropic etching technology that is used to fabricate the V-grooves and the microchannels. Shaped cylindrical microlenses are preloaded and glued into these silicon runners, forming a ladder-like structure consisting of 10 lenses as shown in the photo. The entire 10-lens assembly is then attached to the SiMMs package in a single step. The microlens array serves to collimate the fast axis radiation of the laser diode bars from its original 30° divergence angle into a collimated beam with a divergence angle of <1°.

The backing glass blocks of the SiMMs package are designed to sit side by side on a backplane structure containing cooling water source and drains. The package is specifically designed for close packing to give high effective fill factors. The array shown above has an effective fill fraction of 0.7. This pump module generates 42 kW of pump radiation at an effective irradiance, including the hit from the less than unity fill of the backplane, of 1 kW/cm^2 when viewed in the direction of the emitted radiation. The SiMMs package represents a significant breakthrough in high-power diode-array packaging technology and enables the scaling of power from 2-D diode arrays to100 kW or larger with extremely high brightness. A total of 840 kW arrays have been installed for the heat-capacity laser program. These are the most powerful average-power diode arrays in existence.

Advanced Fiber Lasers for Laser Guide Star Applications and Petawatt Laser Front Ends

Since their "rediscovery" by the University of Southampton in 1985, fiber lasers and amplifiers have steadily increased in importance and output power. They are popular solutions to many problems because they typically have high wall-plug efficiency and are easy to package into robust, reliable turnkey devices that virtually anyone can operate. A cursory analysis of fiber laser development history shows that its average output has been increasing by a factor of 10 every 3 years for roughly the last 18 years and is now reaching output powers of interest to DOE and DoD applications.

Two advanced fiber lasers were investigated by LS&T in 2002: a high-power 938-nm cladding pumped fiber laser to generate 589-nm light for laser guide star application and an ultrastable mode-locked fiber laser as the front end of high-energy petawatt laser system in NIF.

In the laser guide star effort, we are developing a 10-W, compact, all-solid-state laser to be operated at 589 nm. Our design is based on sum-frequency mixing of a 10-W erbium fiber laser (operated at 1583 nm) with a 10-W

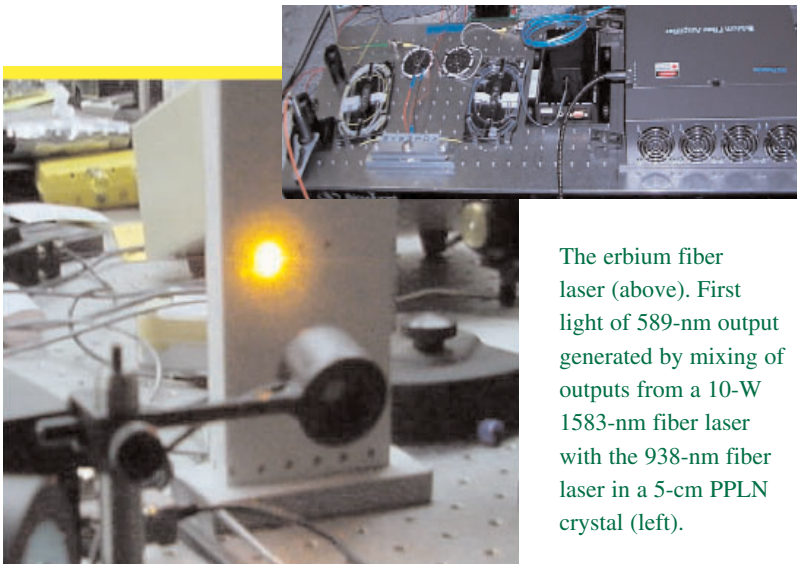

The erbium fiber laser (above). First light of 589-nm output generated by mixing of outputs from a 10-W 1583-nm fiber laser with the 938-nm fiber laser in a 5-cm PPLN crystal (left).

neodymium fiber laser (operated at 938 nm) in a periodically poled nonlinear optical material. We have made significant progress this year. A 10-W erbium fiber laser was successfully assembled using a master oscillator power amplifier configuration. To achieve this output, a 3-mW fiber DFB laser is phase modulated to broaden its linewidth and then amplified in a commercial L-band erbium-doped fiber amplifier.

A cladding pumped neodymium fiber laser was developed and has generated over 2 W of output power. Operation of neodymium-doped glass at 938 nm works best in a nearly pure silica glass, which limits the maximum doping concentration of the neodymium. Fiber lasers are particularly well suited to this application because they are a natural medium for achieving long interaction lengths at high power density. Physics relating to the operation of neodymium at 938 nm were investigated including excited-state quenching as a function of concentration, stimulated Brillouin scattering, ground state absorption, and competition from the1088-nm laser line. The fiber offers a natural mechanism for suppressing light at longer wavelengths as the waveguide is subject to a wavelength-dependent bend loss. By winding the fiber on an appropriately sized mandrel, we were able to create a distributed filter in the gain medium to suppress 1088-nm light and pass 938-nm light. We plan to scale the 2-W 938-nm fiber amplifier to 10-W level in the near future. First light of 589-nm laser was generated by frequency-mixing of outputs from these two fiber lasers (at 1583 nm and 938 nm) in a 5-cm-long periodically poled lithium niobate (PPLN) crystal. We plan to scale the 589-nm output to 10-W level in 2003 for laser guide star application.

We are also developing an advanced fiber laser to be used as the front end for a high-energy petawatt (HEPW) laser system. Our goal is to generate an all-fiber laser source of <200-fs pulses that can be stretched to 3 ns and amplified to output energies to 10 mJ completely within the optical fiber. The effort is divided into three tasks that include (1) construction of the fiber laser mode-locked master oscillator, (2) investigation of a chirped fiber Bragg grating for pulse stretching, and (3) demonstration of a large mode-area optical fiber amplifier, with a specialty refractive index profile designed to amplify and transmit pulses with up to 2.5 times the energy of optical fiber amplifiers with similar core sizes and beam qualities. We have constructed a working prototype of the mode-locked fiber oscillator. We have also designed and procured large-magnitude chirped fiber Bragg gratings for multi-ns pulse stretching. We are continuously investigating the large flattened mode fiber amplifier, with the goal of amplifying laser pulses to energies >10 mJ for HEPW on NIF.

X-Ray Ablation and Neutron Damage Experiments on Optical Materials for IFE

Under the support of the Defense Program's High Average Power Laser Program, LS&T is building a facility, named XAPPER, for x-ray ablation and damage experiments. The primary objective of these experiments is to study pulsed x-ray damage production in candidate inertial fusion energy (IFE) chamber wall (tungsten and carbon composites) and final optic (aluminum and dielectric mirrors, as well as fused silica) materials. XAPPER is also of interest to the heavy-ion fusion program for liquid ablation/condensation studies.

XAPPER (built by PLEX LLC of Brookline, Massachusetts) uses a star pinch to produce soft x-rays. The star pinch is driven by current supplied by six thyratrons that could be switched at 10 Hz or higher. An ellipsoidal condensing optic is used to collect x-rays and bring them to focus on the sample. When oper-

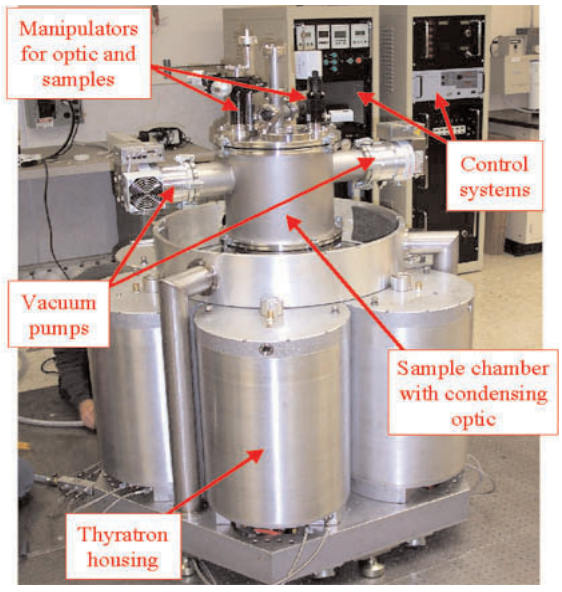

XAPPER facility uses a star pinch to produce soft x-rays at 10 Hz. The star pinch is driven by current supplied by 6 thyratrons.

ated with xenon, XAPPER will provide 113-eV x-rays at fluences of ≥7 J/cm^2. For operation with nitrogen, the peak fluence falls to ~0.25 J/cm^2, but the x-ray energy increases to 430 eV. Use of the condensing optic not only allows for higher fluences, it also greatly reduces the debris loading on the sample. Several million pulses of x-rays can be generated before minor maintenance is required. With x-ray fluence of several J/cm^2 and the short mean free path of the soft x-rays, XAPPER is capable of providing x-ray doses that exceed those expected in laser-IFE power plants. Current diagnostics include a photodiode, a vacuum calorimeter, and an extreme ultraviolet (EUV) spectrometer.

To qualify optical materials for IFE, we have performed a series of radiation experiments on fused silica. The survivability of the final optic, which must sit in the line of sight of high-energy neutrons and gamma rays, is a key issue for any laser-driven IFE concept. Previous work has concentrated on the use of reflective optics. We have introduced and analyzed the use of a transmissive final optic for the IFE application. Neutron damage experiments have been conducted at a range of doses and dose rates, including those comparable to the conditions at the IFE final optic. The experimental work, in conjunction with detailed analysis, suggests that a thin (<1 mm), fused silica Fresnel lens, such as those created for the Eyeglass Project, may be an attractive option when used at a wavelength of 351 nm. Our measurements and molecular dynamics simulations provide convincing evidence that the radiation damage, which leads to optical absorption, not only saturates but that a "radiation annealing" effect is observed. Neutron-induced optical absorption equilibrates at ~5% for a 500-μm-thick fused silica Fresnel lens operated at 300°C. By intentionally operating the optic at an elevated temperature of 500°C, the optical absorption would be reduced to only 0.6%.

Advanced High-Power Lasers for High-Energy Density Plasma Physics Experiments

Under the support of the DOE's NNSA/NV Cooperative Agreement, we are developing a 20 TW / 20 J laser at the Nevada Terawatt Facility of the University of Nevada at Reno to perform high-energy-density plasma physics experiments. The purpose of this laser system is to develop proton and x-ray radiography backlighting techniques, to study plasmas in z-pinches and magnetically insulated transmission lines, and to study deposition of energy from high-intensity laser pulses into plasmas. The performance requirements of this laser are: peak irradiance on target >10^{19} W/cm^2, prepulse irradiance <10^{11} W/cm^2, pointing accuracy of ± 25 μm, timing jitter relative to the Zebra z-pinch facility of <10 ns and shot rate >2/hr. Major efforts were focused on conceptual design of the laser system, which uses an optical parametric chirped-pulse amplifier (OPCPA) for preamplification, and phosphate Nd:glass rod amplifiers for final amplification. A mode-locked Nd:glass oscillator is used to generate 2 nJ, 250 fs-long pulses which are subsequently expanded to 1.5-ns duration using a grating stretcher. Two OPCPA stages will be used to amplify the pulse to 70 mJ. Two double-passed Nd:glass rod amplifiers will provide the final amplification to 30 J. After reflective gratings recompress the pulse to <1 ps, an f/3 off-axis parabolic mirror focuses the beam to a ~10 μm spot. Faraday isolators are used to protect the laser chain from damage. Analysis shows our design meets energy requirements with acceptable nonlinear phase shift and damage margins. The laser system activation is scheduled in 2004.

LS&T is also collaborating with the Physics and Advanced Technologies Directorate (PAT) in an upgrade of the Janus system to achieve 1 kJ in each of its 2 beamlines. Janus is a high-energy Nd:glass laser system operated by PAT to perform high-energy density experiments. The upgraded laser will enable significant new experimental capabilities, including pressures of 20 Mbar, compression to 2–3 times solid density, electron temperatures of >10 keV, and large area shock waves. Major effort was focused on the design of the high-energy amplifiers and beam transport periscopes. Our design codes verified that 1-kJ laser energy could be achieved at the pulse duration of 3 ns, using rod amplifiers, and 10-cm and 15-cm phosphate glass disk amplifiers. The frequency conversion efficiency is expected to be >70%. The installation of the upgraded beamline is scheduled for 2003. When completed, it will provide significant support capability for NIF, including testing and calibrating of diagnostics and training new physicists and engineers to perform high-energy-density experiments.

Solid-State Heat-Capacity Laser for Defense

Under the support of the U.S. Army's Space and Missile Defense Command, and in collaboration with industrial partners including Decade Optical Systems (DOS), General Atomics (GA), PEI Electronics, Northrup/Grumman Polyscientific, and others, we are developing high-average-power (100 kW-class), diode-pumped, solid-state heat capacity laser (SSHCL) technology for applications in tactical short-range air defense missions. As a proof-of-principle, we have built and delivered a 10 kW-class (13 kW actual) heat-capacity laser to White Sands Missile Range. This laser employed flashlamp pumping of the laser media and Nd:glass laser slabs. In order to advance to a 100 kW-class laser, it is necessary to make a transition to laser-diode pumping (for increased power and efficiency), and crystalline laser media (for better thermal characteristics). The baseline design for such a laser uses Nd:doped gallium gadolinium garnet (GGG) as the laser medium and laser-diode pumping at 808 nm.

The technical and engineering basis required for SSHCL have been established. A mobile, compact, lightweight laser system capable of being deployed on a hybrid electric vehicle is currently under development. When complete, this laser system would be capable of defending against short-range rockets, guided missiles, artillery and mortar fire, and unmanned aerial vehicles (UAV). Power for both the vehicle and laser system would come from the vehicle's diesel generator and onboard high-energy lithium ion batteries.

High-Average-Power Pulsed Laser-Material Interaction

The flashlamp-pumped heat-capacity demonstrator laser was delivered to the High Energy Laser System Test Facility (HELSTF) at the White Sands Missile Range in August 2001 and was operated in support of material interaction testing. In its present configuration using a stable optical resonator, it is capable of generating laser pulse energies between 500 and 1000 J/pulse and an average power of up to 13 kW for 10-s burst duration. This combination of high pulse energy at high average power has never been achieved from a solid-state laser system. In 2002, an experimental program was undertaken to study the interaction between this beam and target samples made of aluminum and steel. Detailed numerical modeling was developed to guide the experiments and to help interpret the results. We investigated a number of significant interaction effects that are unique to the high-energy, pulsed-beam format. Initial test data indicate that laser–material interactions under high peak irradiance conditions using a small focusing spot result in rapid penetration due to hydrodynamic forces driven by vaporization. Due to transient surface temperature rise

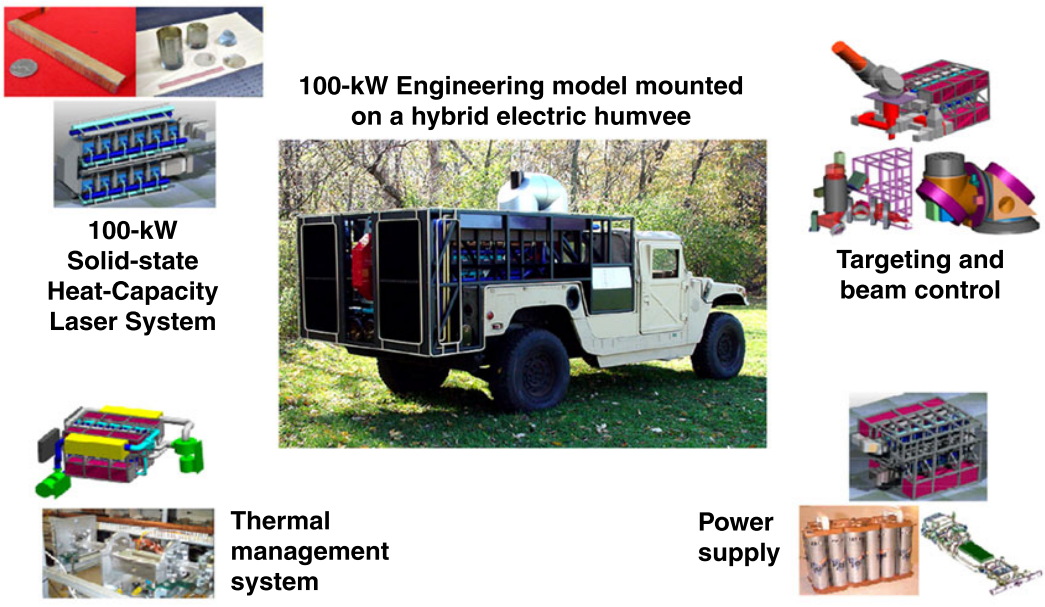

The 100-kW Solid-State Heat-Capacity Laser will have a 10% electrical efficiency, and the required 1-MW input is supplied by the vehicle traction battery mounted on a conceptual system using a hybrid electric humvee.

Courtesy of General Atomics and PE1 Electronics.

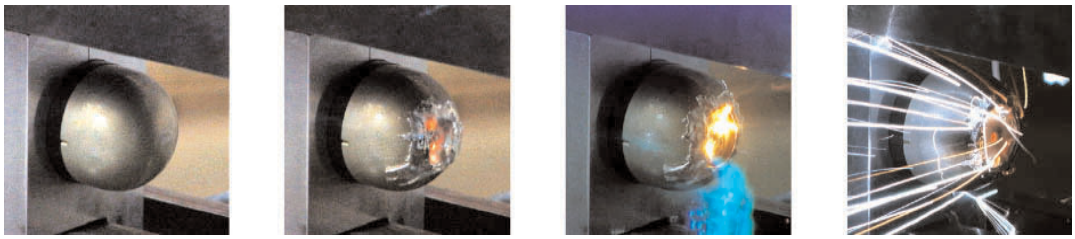

Frames taken from a movie showing the interaction of the laser beam with a steel coupon. The beam has punched through the coupon at this point.

during each laser pulse, increased heating over that achieved from a CW laser of the same average power is observed. High peak surface temperatures during each laser pulse also drive the combustion of the metal target under high-speed air flow conditions, providing additional energy deposition and heating.

In 2002, we had the opportunity to irradiate an antitank guided munition (ATGM) with the 10-W SSHCL. A video sequence of the actual ATGM crushing is shown above. The crush fuse on the ATGM is made from an aluminum alloy. The mechanism used to trigger the ATGM fuse was straightforward. The nose of the ATGM is a crush switch consisting of inner and outer domes. When heated by the laser, the fuse is weakened and collapses under the aerodynamic air flow load. When the two domes contact, the fuse is activated. The total fluence required to compromise the ATGM was 702 J/cm^2, a figure almost 10 times less than the value that has been used in the battlefield simulations using an existing Directed Energy (DE) laser system.

Adaptive Resonator Control for High Beam Quality Operation

Low divergence is necessary to propagate a high-average beam from an SSHCL to target. To do this, the relatively small thermally induced optical distortions in the heat-capacity amplifier of the laser system must be corrected. An unstable resonator that incorporates an intracavity deformable mirror has been incorporated to make these corrections. LS&T successfully demonstrated lasing from an SSHCL with wavefront correction using the 3-slab flashlamp-pumped testbed amplifier. A new mirror, built to tighter specifications was developed to achieve wavefront correction at full average power. A complete understanding of the impact of small-scale structure (ripple) of only 25 nm rms is now in hand and a combination of laboratory measurements and numerical simulation has validated a new mirror design. We have recently demonstrated <1.5 times the diffraction-limited divergence in active lasing low-energy experiments using a full-scale resonator and 3-slab flashlamp-pumped amplifier with the original deformable mirror. The full 10-kW amplifier head has now been returned from HELSTF to LLNL where it is being integrated with the adaptive resonator to demonstrate high-beam-quality operation for a 10-s burst at full power.

Diode-Pumped 3-Slab Nd:GGG Amplifier

The scaling from the 10-kW flashlamp-pumped demonstrator laser to 100-kW will use diode-pumped neodymium-doped gadolinium gallium garnet (Nd:GGG) as gain medium. LS&T is building a 3-slab amplifier testbed as the first conceptual submodule of the 100-kW laser design. The 3-slab testbed will use three full-aperture Nd:GGG crystals. To establish a solid technical basis for such a laser, we are also developing a half-scale testbed that utilizes a single Nd:GGG slab with an active region measuring 5 × 10 cm^2 in size and pumped by four half-size laser diode arrays. The diode arrays consist of 28 SiMMs (Silicon Monolithic Microchannels) “tiles” arranged in a 4 × 7 configuration that produce an average optical power of 4.2 kW/array. The pulse width is nominally 500 µs. We performed a series of experiments to verify the design of the100-kW SSHCL system with respect to pulse energy, efficiency, and run time. Optical gain coefficient, pump uniformity, output wavefront, and temperature rise in the lasing medium were also measured to benchmark the temperature-dependent energetic model.

Using a stable resonator with low output coupling, we obtained kW output from the half-scale system. At 200 Hz, over a 10-s run, we achieved an average power of 2.8 kW with an initial output in excess of 3 kW. The average diode-array optical pump power used for this experiment was 13.3 kW, and the overall diode electrical efficiency was 45%. Initial

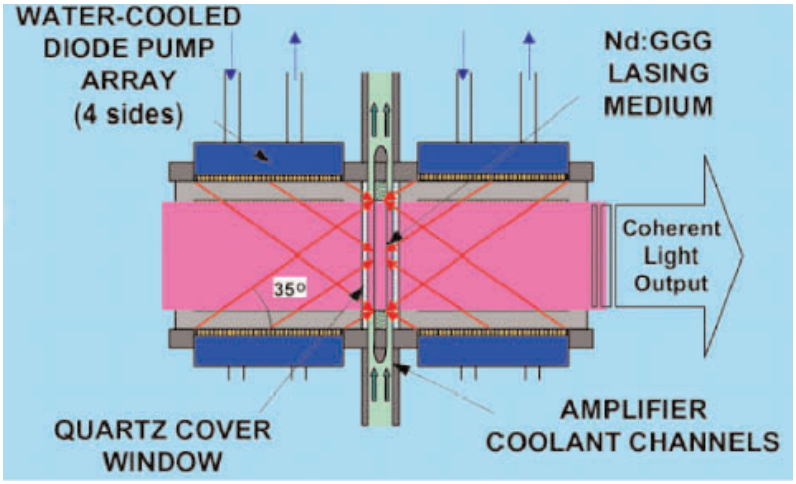

Schematic of the half-scale SSHCL. This is the fundamental building block of the diode-pumped Nd:GGG laser system.

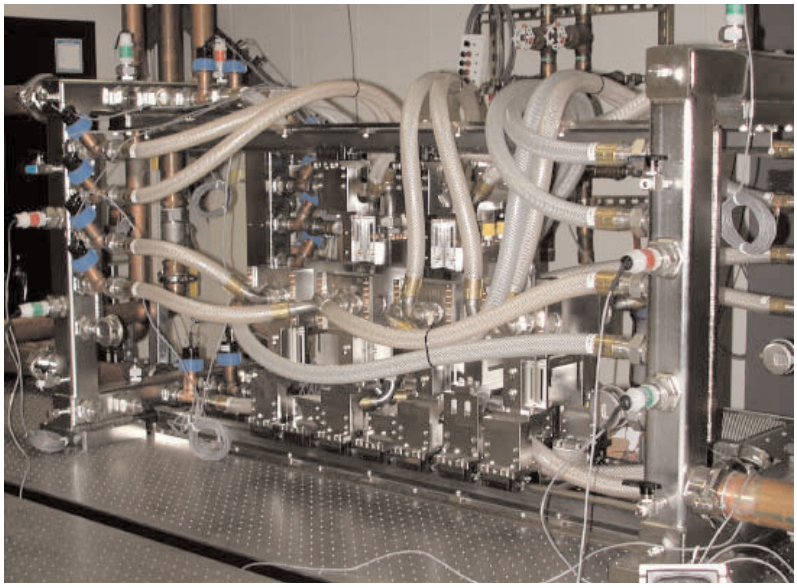

Installed 3-slab diode-pumped SSHCL head assembly hardware.

laser testing has demonstrated 9% electrical-to-optical efficiency, a figure very near the 10% goal designed for the 100-kW mobile laser system.

Using the output beam from the half-scale system, we were able to penetrate a 1.5-mm-thick steel coupon in a matter of a few seconds. The mechanical structure of the 3-slab testbed is nearing completion, and the diode-array thermal management system is fully activated. Six of the required 12 full-scale diode arrays (80-kW peak each) manufactured by Armstrong Laser Technology have been tested and qualified. Six additional arrays have been manufactured and are undergoing testing.

Fabrication of the three Nd:GGG slabs, including diffusion-bonded edge cladding and optical coating, is complete. We plan to activate the three-slab diode-pumped Nd:GGG testbed in 2003 as a scientific prototype for the 100-kW system to be developed for battlefield defense. It is anticipated that this system will generate an output power in excess of 15 kW—greater than the nine-slab flashlamp-pumped system currently in operation at the Army's HELSTF.

For the first time we have now demonstrated high-efficiency operation of a diode-pumped Nd:GGG SSHCL and are poised to operate the first conceptual submodule of a 100-kW objective laser system.

Material Processing Using Pulsed Solid-State Lasers

Laser peening is an emerging surface treatment technology for metals that places deep residual compressive stress into the surface, greatly improving resistance to fatigue failure and stress corrosion cracking. A laser system appropriate for peening at an industrial level requires an average power in the hundred-watt to kilowatt range, a pulse energy of around 25 to 100 J per pulse and a pulse duration of 10 to 30 ns. A solid-state laser with such capability was first developed for a DoD mission in 1996 by Drs. Lloyd Hackel and Brent Dane of LLNL. In order to complete the chain required for technology commercialization, we successfully established a Cooperative Research and Development Agreement (CRADA) with the Metal Improvement Company (MIC) of Parnasus, NJ. During the past year, we demonstrated key process performance, supported assembly of several high-rate, production-type laser-peening systems, and MIC began peening of commercial jet engine components. LS&T is currently developing the laser peening process to improve fatigue and corrosion lifetimes of metals and alloys in several project areas: (1) for DoE's Civilian Radioactive Waste Management System program, Yucca Mountain Project (YMP), to improve the service lifetime of metal canisters designed for long-term disposal of high-level radioactive waste generated by commercial nuclear power plants and government reactors, (2) for the U.S. military to improve the fatigue lifetime and reliability of aircraft structures as well as gears, bearings, and drive trains used in rotorcraft and combat vehicles and other

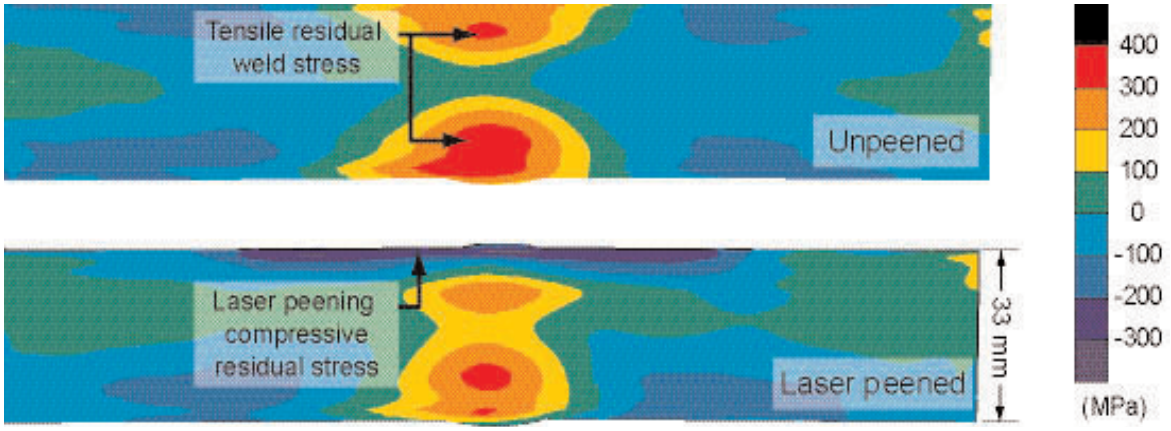

Results of contour residual stress measurement in a peened and unpeened Alloy 22 weld. Laser peening turned high tensile residual stress into near-yield-level compressive residual stress at the part surface.

energy-generation equipment in the DoD's weapon system, (3) for oil and gas exploration and production, to improve the performance and reliability of structural materials. Spin-off technologies also demonstrate that pulse lasers are making an impact on U.S. industry in general; for example, technology like laser peen-marking, which provides an easy way to identify parts, and peenforming, which enables complex contouring of problematic thick metal components such as parts of large aircraft wings. We have recently partnered with the Material Performance Laboratory at the University of California, Davis, to further the development of laser peening.

Laser Peening Improves Corrosion Resistance and Mitigates Tensile Residual Stresses in Alloy 22

Under the support of Bechtel SAIC, and in collaboration with UC Davis and Metal Improvement Company, we are developing a laser peening process for application to radioactive waste storage. DOE has been charged with designing, constructing and operating a facility at the Yucca Mountain Project's (YMP) Nevada site to permanently store the nation's high-level civilian and military radioactive waste. In addition to the natural barriers at the Nevada site, a number of engineered barriers are being designed to help the facility meet its containment goal. Foremost among these is the waste package, which will be fabricated from Alloy 22, which is one of the materials known to be most highly resistant to corrosion. Our current work has focused on mitigating the potential for stress corrosion cracking (SCC) by eliminating the near-surface tensile residual stresses resulting from welding processes and evaluating the corrosion resistance of laser-peened Alloy 22.

Parametric studies covering many of the laser peening conditions have resulted in an improved treatment plan and the deepest residual stresses we have produced to date. Examples of two-dimensional residual stress fields in peened and unpeened Alloy 22 weldments, measured with the contour method, are shown above.

The effects of laser peening are dramatically demonstrated, with the near-surface longitudinal (along the weld) tensile residual stress present in the unpeened plate converted into deep, compressive residual stress with the application of laser peening.

Measurements of residual stress were made for various coupon thickness (from 5 to 35 mm). The depth of compressive residual stress appears to increase with coupon thickness.

These depths of residual stress, on the order of 20% of the part thickness for the range tested, far exceed the capabilities of conventional shot peening and other methods used in industry. This deep compressive stress serves to inhibit the process of SCC, which occurs in a tensile stress field. We have also measured the corrosion rate of peened and unpeened Alloy 22 coupons. Preliminary results have shown that laser-peened Alloy 22 will corrode more slowly than Alloy 22 alone. Because of the large depth of residual compressive stress, laser-peened material will continue to inhibit SCC even after several millimeters of material are removed through general corrosion. These beneficial characteristics, in conjunction with

its noncontact, "hands off" nature, make laser peening a good candidate for YMP to improve the corrosion resistance and lifetime of storage canisters.

Laser Peening Improves Fatigue Life of Aluminum Components for USAF

Under the support of the United States Air Force's (USAF's) Aging Landing Gear Life Extension Program, LS&T is working with UC Davis, the Ogden Air Logistics Center Landing Gear Engineering Branch (OO-ALC/LILE), and Metal Improvement Company, Inc. (MIC) to evaluate the advantages of applying laser peening (LP) to improve the performance of landing gear components for the USAF. Using test coupons made from the same high-strength aluminum alloy (7049-T73) as the trunnion, we systematically studied the effects of laser peening on the fatigue life and SCC characteristics of a trunnion, which is a part of the main landing gear on the USAF's T-38 aircraft. The results clearly show that laser peening can significantly improve the fatigue life of this component and its resistance to SCC.

Since the trunnions are currently treated with a shot peening (SP) treatment, an additional goal of this study was to compare the two surface treatments (LP and SP) and to also investigate the potential effects of applying laser peening to previously shot-peened specimens. Fatigue tests at various load levels near the service stress were performed. All three surface treatment techniques (laser peening LP, shot peening SP, and laser peening on top of the shot peening process LS+SP) increased the fatigue life of the test specimen but the greatest benefits appear to come from the laser peening treatment. Additionally, the benefits of each of the surface treatments increased at longer fatigue lives (lower maximum stress).

Stress corrosion cracking tests were performed on C-ring specimens made from 7075-T6 aluminum. The same surface treatments as above were used for the SCC tests (LP, SP, SP+LP) along with a control case of no surface treatment. The untreated C-ring specimens all showed clear evidence of SCC and cracked in half in the caustic environment after a few days (11, 13, and 23 days) while none of the treated specimens cracked throughout the entire test duration of 60 days. Although this test was not conclusive in ranking the benefits of LP over SP with regard to SCC, it did clearly show that LP is an effective tool to enhance the SCC performance of untreated specimens.

We are currently performing similar laser peening and fatigue tests on actual T-38 trunnions. Since the fatigue coupons were specifically designed to have a fatigue performance similar to the T-38 trunnion, it is expected that a similar life extension is achievable on the actual part. The estimated cost savings to the USAF (due to a reduction in the replacement costs and maintenance and inspection time) will be on the order of tens of millions of dollars.

Commercialization of Laser Peening Process and Tool

While the YMP and USAF development work continues, laser peening was also introduced this past year into commercial production by Metal Improvement Company, our CRADA partner. The laser peening system was deployed to solve an important fatigue failure problem in high-value commercial jet engine components. Since commercial introduction in May 2002, aircraft worth billions of dollars are now in service with laser-peened parts—saving millions of dollars per month in aircraft maintenance costs, millions more in parts replacement costs, and all the while greatly enhancing safety.

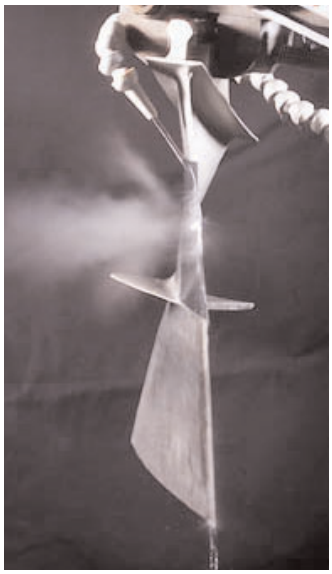

Laser peening is being applied to eliminate fatigue failure in high-value commercial jet engines.

SELECTED PAPERS PUBLISHED IN 2002

Adams, J. J., and Ebbers, C. A., Linear Electro-Optic Properties of YCa4O(BO3)3.

Bayramian, A. J., Beach, R. J., Behrendt, W. C., Bibeau, C., Campbell, R. W., Dixit, S. N., Ebbers, C. A., Freitas, B. L., Kanz, V. K., Rushford, M. C., Payne, S. A., Schmidt, J. R., Schaffers, K. I., Skulina, K. M., Telford, S., Tassano, J. B., Activation of the Mercury Laser, a Diode-Pumped, Gas-Cooled, Solid-State Slab Laser.

Bayramian, A. J., Beach, R. J., Behrendt, W. C., Bibeau, C., Ebbers, C. A., Freitas, B. L., Kanz, V. K., Payne, S. A., Schaffers, K. I., Skulina, K. M., Smith, L. K., Tasano, J. B., Van Lue, D., Initial Experiments on Mercury, a 100-J/10-ns/10-Hz/10% Efficiency Diode-Pumped, Solid-State Laser.

Beach, R. J., Feit, M. D., Mitchell, S. C., Cutter, K. P., Payne, S. A., Mead, R. W., Hayden, J. S., Krashkevich, D., Alumni, D. A., Phase-Locked Antiguided Multiple-Core Ribbon Fiber.

Bennett, G. R., Cuneo, N. E., Vesey, R. A., Porter, J. L., Adams, R. G., Aragon, R. A., Caird, J. A., Landen, O. L., Rambo, P. K., Rovang, D. C., Ruggles, L. E., Simpson, W. W., Smith, I. C., and Wenger, D. F., Symmetric Inertial-Confinement-Fusion-Capsule Implosions in a Double-Z-Pinch-Driven Hohlraum.

Boley, C. D., and Rubenchik, A. M., Modeling of High-Energy Pulsed Laser Interactions with Coupons.

Britten, J. A., Bryan, S. J., Summers, L. J., Nguyen, H. T., Shore, B. W., Large Aperture, High-Efficiency Multilayer Dielectric Reflection Gratings.

Caird, J. A., Beer, G. K., Erlandson, A. C., Mills, S. T., Murray, J. E., Nostrand, M. C., Roberts, D. H., Skulina, K. M., Weiland, T. L., Wegner, P. J., 1.5-kJ Nd:glass Laser System for Large Area Damage Testing.

Chen, H. L., Evans, K. J., Hackel, L. A., Rankin, J. E., Yamamoto, R. M., Mitigation of Tensile Weld Stresses in Alloy 22 Using Laser Peening.

Dawson, J. W., Beach, R. J., Jovanovic, I., Wattellier, B., Liao, Z., Payne, S. A., Barty, C. P., Large Flattened Mode Optical Fiber for High Output Energy Pulsed Fiber Lasers.

Dawson, J. W., Drobshoff, A.D., Liao, Z., Beach, R. J., Pennington, D. M., Payne, S. A., High-Power 938-nm Cladding Pumped Fiber Laser.

Erlandson, A. C., Batie, S., Bauer, B., Caird, J. A., Ebbers, C. A., Glassman, J., Ivanov, V., LeGalloudec, B., LeGalloudec, N., Letzring, S., Payne, S. A., Stuart, B. C., Design of a 20-TW/20-J, Chirped-Pulse Amplification Laser for High-Energy-Density Plasma Physics Experiments at the University of Nevada at Reno.

Feit, M. D. and Rubenchik, A. M., Mechanisms of CO2 Laser Mitigation of Laser Damage Growth in Fused Silica.

Feit, M. D. and Rubenchik, A. M., Analysis of Raster Scanning Damage and Conditioning Experiments.

Jovanovic, I., Comaskey, B. J., Ebbers, C. A., Bonner, R. A., Pennington, D. M., and Morse, E. C., Optical Parametric Chirped-Pulse Amplifier as an Alternative to Ti:sapphire Regenerative Amplifiers.

Jovanovic, I., Dixit, S. N., Wattellier, B., Hermann, M. R., Barty, C. P., Feasibility Study of Thin Fresnel Lens Use in Multi-kJ, Short-Pulse Laser Systems.

Kim, B. M., Komashko, A. M., Rubenchik, A. M., Feit, M. D., Reidt, S., Da Silva, L. B., Eichler, J., Pressure Wave Generation and Energy Balance in Ultrashort Laser Pulse Surface Ablation of Water.

Nakano, H., Kanz, K., and Ebbers, C. A., A Thermally Compensated, Dueterated KDP Q-Switch for High Average Power Lasers.

Nelson, A. J., van Buuren, T. W., Schaffers, K. I., Terminello, L. J., Photoemission and Photoabsorption Investigation of the Electronic Structure of Ytterbium-Doped Strontium Fluoroapatite.

Pennington, D. M., Hermann, M. R., Barty, C. P., Caird, J. A., Clark, W. J., Dawson, J. W., Erlandson, A. C., Jovanovic, I., Key, M. H., Skulina, K. M, Wattellier, B., Conceptual Design for a High-Energy Petawatt Laser on the National Ignition Facility.

Prasad, R. R., Bruere, J. R., Peterson, J., E., Halpin, J. M., Auyant, L., and Borden, M. R., Conditioning and Mitigation of Tinsley, Inclusion-Free, Wedged Focus Lens.

Rankin, J. E., Hill, M. R., and Hackel, L. A., The Effects of Process Variations on Residual Stress in Laser-Peened 7049 T73 Aluminum Alloy.

Schaffers, K. I., Tassano, J. B., Bayramian, A. B., Morris, R. C., Growth of Yb: S-FAP [Yb3+:Sr5(PO4)3F] Crystals for the Mercury Laser.

Yu, J., Britten, J. A., Summers, L. J., Dixit, S. N., Hoaglan, C. R., Aasen, M. D. , Hackel, R. P., Prasad, R. R., Fabrication of Beam Sampling Gratings for the National Ignition Facility.

Wattellier, B., Jovanovic, I., Barty, C. P., Cascaded Optical Parametric Amplification for Extreme Contrast Enhancement.

Wynne, A. E., and Stuart, B. C., Rate Dependence of Short-Pulse Laser Ablation of Metals in Air and Vacuum.

DISCLAIMER

This work was performed under the auspices of the U.S. Department of Energy by University of California Lawrence Livermore National Laboratory under Contract W-7405-ENG-48.

This report has been reproduced directly from the best available copy.

Available to DOE and DOE contractors from the
Office of Scientific and Technical Information
P.O. Box 62, Oak Ridge, TN, 37831
Prices available from (615) 576-8401, FTS 626-8401

Available to the public from the National Technical Information Service,
U.S. Department of Commerce, 5285 Port Royal Rd., Springfield, VA 22161

March 2003

UCRL-ID-134972-02